International Journal of Greenhouse Gas Control 134 (2024) 104129

Contents lists available at ScienceDirect

International Journal of Greenhouse Gas Control

journal homepage: www.elsevier.com/locate/ijggc

A holistic framework for evaluating gigaton scale geological CO_2 storage applied to the Alberta oil sands: Physics, policy, and economics

Yu Hao Zhao [a], Nima Shakourifar [a], Negar Shahsavar [a], Yaxuan Lei [b], Benzhong Zhao [a,*]

[a] Department of Civil Engineering, McMaster University, 1280 Main Street West, Hamilton, ON, L8S 4L7, Canada
[b] Bonnefield Financial Inc., 141 Adelaide Street West #510, Toronto, ON, M5H 3L5, Canada

ARTICLE INFO

Keywords:
Net-zero emissions
Carbon sequestration
Oil sands
Storage capacity
Government policy
Economic feasibility

ABSTRACT

Carbon capture, utilization, and storage (CCUS) is capable of significantly reducing anthropogenic carbon dioxide (CO_2) emissions. In the Canadian context, CCUS is an important tool in mitigating emissions in the oil and gas sector, which is a significant contributor of greenhouse gas emissions in Canada. Previous studies have demonstrated the viability of CCUS in the Alberta oil sands but have not considered all the critical factors impacting the success of a CCUS system including the availability of emission sources, the design of a CO_2 transportation network, the availability and capacity of suitable storage sites, the long-term fate of injected CO_2, the economic viability of the system, and the overall policy environment. We consider all these factors in proposing a CCUS hub that captures CO_2 from a cluster of 10 large oil sands emitters for permanent storage in the Devonian Nisku and Wabamun saline aquifers. We forecast the oil sands emissions using a logistic model and simulate the pressure evolution and CO_2 plume migration to show that the aquifers can safely store the entirety of forecasted emissions, which amounts to over 1.9 gigatons by the end of the century. We design a pipeline network connecting the emitters and the storage formations, which is estimated to cost approximately $ 4-billion. We consider both privately-funded and publicly-funded scenarios for financing the pipeline network, taking into account relevant financial and policy incentives. Our work outlines the key points that must be considered when designing a large-scale CCS system, namely availability of emission sources, efficiency of pipeline route, storage capacity and injectivity, CO_2 migration and trapping, cost, and policy and financial incentives. This provides a comprehensive framework upon which future CCUS projects can be evaluated to ensure its long-term viability and success.

1. Introduction

Climate change mitigation has gained momentum in recent years as the devastating effects of climate change have become increasingly evident. The focus of climate change mitigation is to reduce the amount of greenhouse gas (GHG) emissions into the atmosphere (Anderson and Newell, 2004; Rockström et al., 2009), which has increased by more than 39% over the past century (Leung et al., 2014) and is directly responsible for climate change (Falkowski et al., 2000; Hansen and Sato, 2004; Haszeldine, 2009; Kennedy et al., 2009). The Paris Agreement (United Nations, 2015) formalizes a global commitment to limit overall global temperature increases to 1.5–2 °C through drastic reductions in GHG emissions. As a signatory to the Paris Agreement, Canada is committed to reducing its annual GHG emissions by 30% of 2005 emission levels by 2030 (Environment and Climate Change Canada, 2021d). More recently, Canada further increased its emissions reduction commitment to 40%–45% of 2005 levels in the 2021 Nationally Determined Contribution (NDC) (Environment and Climate Change Canada, 2021b). Canada emitted 730 megatonnes (Mt) of GHG in 2005 and is projected to emit 468 Mt of GHG in 2030 (Environment and Climate Change Canada, 2021b,a). Therefore, Canada needs to sequester 30–67 Mt of GHG per year by 2030 to satisfy the NDC commitment.

GHG emissions in Canada belong to six main sectors as defined by the Intergovernmental Panel on Climate Change (IPCC), which include Energy - Stationary Combustion Sources, Energy - Transport, Agriculture, Energy - Fugitive Sources, Industrial Processes and Product Use, and Waste. Each of these sector accounts for 44%, 30%, 8.1%, 7.4%, 7.4%, and 3.8% of 2019 emissions, respectively (Environment and Climate Change Canada, 2021c). The Energy - Stationary Combustion sector emitted 319 Mt of GHG in 2019 (Environment and Climate Change Canada, 2021c), and it is by far the largest emitter in the Canadian economy. More specifically, Oil and Gas Extraction, a

* Corresponding author.
E-mail address: robinzhao@mcmaster.ca (B. Zhao).

https://doi.org/10.1016/j.ijggc.2024.104129
Received 25 September 2023; Received in revised form 20 January 2024; Accepted 3 April 2024

subcategory within the Energy - Stationary Combustion sector, emitted 105 Mt of GHG in 2019, which equates to 14% of total Canadian emissions (Environment and Climate Change Canada, 2021c). The Canadian oil and gas sector is projected to account for 27% of national GHG emissions by 2030 (Environment and Climate Change Canada, 2021a).

Carbon capture, utilization and storage (CCUS) is a proven technology that is capable of significantly reducing anthropogenic carbon dioxide (CO_2) emissions (Boot-Handford et al., 2014; Bui et al., 2018; Edwards and Celia, 2018; Lackner, 2003; Orr, 2009; Pacala and Socolow, 2004; Szulczewski et al., 2012). In CCUS, CO_2 is captured at stationary point sources and utilized in industrial processes, including enhanced oil recovery, before it is stored. A subset of CCUS is carbon capture and storage (CCS), where the captured CO_2 is directly injected underground for permanent storage. The widespread adoption of CCS has great potential for emission reduction (Metz et al., 2005; Leung et al., 2014), and (Metz et al., 2005) estimates that CCS can account for up to a third of global emissions reductions by 2095 under certain scenarios. CCS is especially suited to industrial processes (Osman et al., 2021) whose emissions are from concentrated point sources that can be readily captured (Metz et al., 2005; Raza et al., 2019). The implementation of large-scale CCS is critical in the GHG emission reduction effort in Canada, especially in the Province of Alberta, which houses many industries with significant GHG emissions.

There are currently two operational CCUS projects in Alberta, namely the Quest Carbon Capture and Storage Project and the Alberta Carbon Trunk Line (ACTL) system. The Quest project captures CO_2 from the Shell Scotford Upgrader, a mined oil sands extraction facility, and transports it to the Basal Cambrian Sands saline aquifer for storage (Alberta Department of Energy, 2020). This project stores around 1 Mt of CO_2 per year (Duong et al., 2019) and it will reach a cumulative volume of 27 Mt stored by the end of the project lifespan (Alberta Department of Energy, 2020). At a larger scale, the ACTL system collects CO_2 from industrial emitters near Edmonton, Alberta and transport it to central Alberta for use in enhanced oil recovery before permanent storage in the Nisku and Leduc formations. Currently, the ACTL captures 1.6 Mt of CO_2 annually, which will increase to 14.6 Mt of CO_2 annually at full capacity (Cole and Itani, 2013). These projects have successfully demonstrated the feasibility of CCUS in Alberta. However, even at the maximum design capacity, they fall short of the ambitious target stipulated in the most recent NDC. Therefore, significant increases in CCUS capacity is urgently needed to achieve Canada's emission reduction goals. To this end, the Government of Canada has committed to developing a comprehensive CCUS strategy (Environment and Climate Change Canada, 2020, 2021b, 2022) and is developing an investment tax credit for capital investment in large-scale CCS projects (Environment and Climate Change Canada, 2021b, 2022; Department of Finance Canada, 2022). The federal government believes that Canada has a comparative advantage in CCUS technology and has reaffirmed its commitment to advancing the deployment of CCUS in the most recent climate action plan (Environment and Climate Change Canada, 2022). The province of Alberta has also announced its intention to establish carbon sequestration hubs that include multiple industrial emissions sources (Government of Alberta, 2021). Clearly, there is a need to expand the CCUS capacity in Alberta and strong support at both the federal and provincial levels.

The feasibility of expanding CCUS in Alberta has been examined in previous studies. Eisinger et al. (2011) studied the possibility of sequestering CO_2 from coal-fired power plants in geological formations in the Wabamun Lake area, with particular focus on CO_2 injection in the Nisku formation. Jensen et al. (2013) proposed a pipeline network connecting industrial sites in the Plains CO_2 Reduction (PCOR) Partnership region, which includes Alberta. They showed that sufficient CO_2 sources exist in the region to support a CO_2 pipeline. Bachu et al. (2014b) studied the feasibility of CO_2 storage in deep Devonian saline aquifers located west of the Athabasca region in Alberta. They applied a volumetric method using aquifer characteristics and applied the regulatory constraint that CO_2 storage depth must be greater than 1000 m (Government of Alberta, 2011) to estimate the potential storage capacities of 10 aquifers. Specifically, they multiplied the total pore volume of the aquifers by a simple storage efficiency coefficient (Goodman et al., 2011) to arrive at the storage capacity estimates. Bachu (2007, 2015) recommended that estimations of storage capacities on a local scale be modelled numerically to account for the dynamic factors affecting storage capacity as well as site-specific characteristics such as the number and configuration of injection wells.

The existing studies demonstrated the general feasibility of CCUS expansion in Alberta. However, they only considered one aspect of the overall system. CCUS is a complex public works project that requires careful consideration of many factors, including the availability of emissions sources (Hasan et al., 2015; Tapia et al., 2018; Yu et al., 2019), the availability of suitable storage sites (Budinis et al., 2018; Ciotta et al., 2021; Szulczewski et al., 2012), the safety during injection and long-term fate of the CO_2 (Szulczewski et al., 2012), the design of a CO_2 transportation network (Balaji and Rabiei, 2022; Jensen et al., 2013), the economic viability of the project (Edwards and Celia, 2018; Leonzio et al., 2019; Tapia et al., 2018; Yao et al., 2018), and a suitable policy environment (Bäckstrand et al., 2011; Alcalde et al., 2019; Romasheva and Ilinova, 2019).

Here, we propose a new CCS system in Alberta that will store over 1.9 gigaton (Gt) of CO_2 over its lifetime. We demonstrate that a holistic approach is necessary in planning CO_2 storage at the gigaton-scale, which includes future emission projections, emission capture and transport, pressure and migration capacity of the storage aquifer, the costs and financing required, and the regulatory and policy environment. This holistic approach is essential due to the interdependent nature of these elements — future emissions projection determines the selection of suitable aquifers, the number and location of injection wells to prevent fracturing the aquifer and limit CO_2 migration, which then dictates the length and size of the CO_2 transport pipeline, and the overall cost of building the necessary infrastructure. Finally, such a large-scale project can only take place under a hospitable regulatory and policy environment.

Our proposed CCS system transports CO_2 from a dense cluster of emitters in the Athabasca oil sands region to deep saline aquifers for permanent storage. We design the route of the pipeline network to connect the cluster of emitters to the Nisku and Wabamun formations following the shortest and thus most efficient path. We project the future capturable annual emissions of the cluster using a logistic growth model, which adds up to over 1.9 Gt for the remainder of the century. To ensure this amount of CO_2 can be safely stored at the Nisku and Wabamun formations, we model the pressure evolution within the saline aquifers during the injection period and find that the pressure increase does not exceed the regulatory limit. In addition, we model the post-injection evolution of the CO_2 plume, considering the relevant trapping mechanisms. We find that the CO_2 plume will be fully trapped via residual trapping and solubility trapping before reaching the 1000 m depth contour line. We note significant uncertainties in the aquifer properties, and that our analysis is conducted using representative values based on available information. Using the representative values, we estimate the total capital cost of the CO_2 pipeline network. We also identify implications for policymakers, including policy changes and governmental incentives that would improve the financial viability of large-scale CCS projects in Canada.

2. Emission source

The Athabasca oil sands region hosts a number of concentrated large CO_2 emitters, which is attractive for the implementation of large-scale CCS.

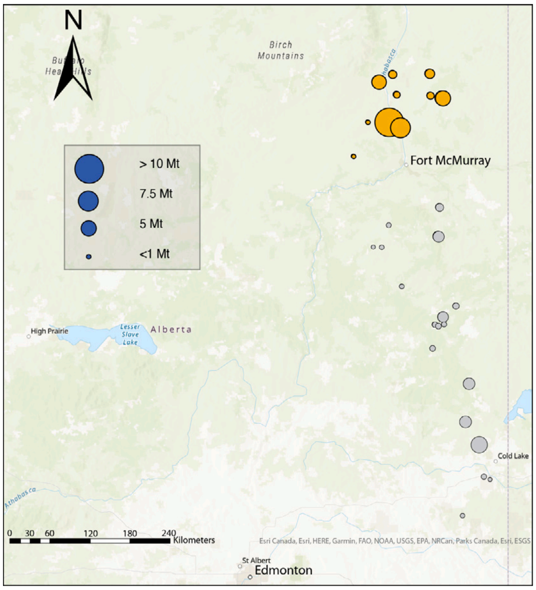

Fig. 1. The circles represent facilities with large GHG emissions in the Athabasca oil sands region. The size of each circle is proportional to the facility's GHG emissions in 2018. We identify a hub of 10 facilities (yellow) north of Fort McMurray as particularly attractive for large-scale CCS due to their spatial proximity.

2.1. Emission clusters

The implementation of CCS is more attractive to facilities emitting large amounts of emissions due to economies of scale. The Government of Alberta defines large emitters as those with annual GHG emissions of greater than 0.1 Mt in the Technology Innovation and Emissions Reduction (TIER) Regulation (Government of Alberta, 2020). We follow this definition and identify the list of oil sands facilities with greater than 0.1 Mt of GHG emissions in 2018 from the Canadian Greenhouse Gas Reporting Program (GHGRP) (Government of Canada, 2021b). The CNUL Peace River Complex, AOC Hangingstone SAGD, and Scotford Upgrader and Upgrader Cogeneration facilities are excluded since they are located far away from the other facilities, which makes their inclusion in a CCS network economically unviable. We arrive at a list of 29 oil sands facilities (Fig. 1). From these 29 facilities, we highlight a dense cluster of large emitters north of Fort McMurray which consists of 10 facilities with annual emissions of 37.8 Mt in 2018 (Fig. 1). This represents 53% of the total Alberta oil sands emissions from large-scale emitters. We study the feasibility of building a CCS system around this cluster of 10 emitters, which we refer to as the CCS hub in the remainder of the paper. The spatial proximity and large CO_2 footprint of this cluster of emitters is particularly attractive for large-scale CCS due to great economies of scale (Ringrose et al., 2021).

2.2. Carbon capture technology

There are three major potential forms of carbon capture for use in the oil sands: pre-combustion, post-combustion, and oxy-fuel combustion. We propose the use of post-combustion carbon capture (PCCC) because it is the most widely used technology at a global scale (Chao et al., 2021), and it can be readily implemented at existing oil sands facilities (MacDowell et al., 2010; Mokhtar et al., 2012; Zanco et al., 2021). Although PCCC technology has a high heat requirement (Ashrafi et al., 2021), it nevertheless possesses several advantages over other forms of carbon capture technology. Specifically, pre-combustion carbon capture must be integrated closely with the CO_2 source, while oxy-fuel combustion has a higher capture cost per tonne compared to PCCC (Skagestad et al., 2014). Meanwhile, PCCC has already been demonstrated at the commercial scale (Bui et al., 2018; Liang et al., 2015), and it is regarded as the most mature technologies due to its applicability across a range of sectors (Ashrafi et al., 2021). Furthermore, PCCC has a relatively low cost per unit captured compared to other technologies (Mokhtar et al., 2012). Ashrafi et al. (2021) showed that part of the energy required by PCCC could be produced using excess heat available in the flue gas of steam-assisted gravity drainage (SAGD) facilities, which are projected to comprise the majority of future emissions from the oil sands (Ordorica-Garcia et al., 2011). This waste heat recovery could reduce the gross heat requirement of PCCC and thus both fuel requirement and cost (Ashrafi et al., 2021).

Two main forms of PCCC technology are applicable to oil sands facilities: a solid adsorbent and an amine-based solvent (Ashrafi et al., 2021). Adsorbent-based technology has the advantages of being more stable and long-lasting without the need to replace solvent, while solvent-based technology is more proven commercially and has a higher technology readiness level (Ashrafi et al., 2021). Both forms of PCCC have a capture efficiency of 90% (Ordorica-Garcia et al., 2011; Pilorgé et al., 2020; Porter et al., 2017; Zanco et al., 2021) and are considered ready for commercialization (International Energy Agency, 2020; Kazemifar, 2021). Ordorica-Garcia et al. (2011) found that approximately 88% of CO_2 emissions from oil sands operations are amenable to PCCC, since emissions from operations including on-site transportation and maintenance cannot be captured. Therefore, the ratio between capturable emissions and total oil sands emission is $R \approx 79\%$.

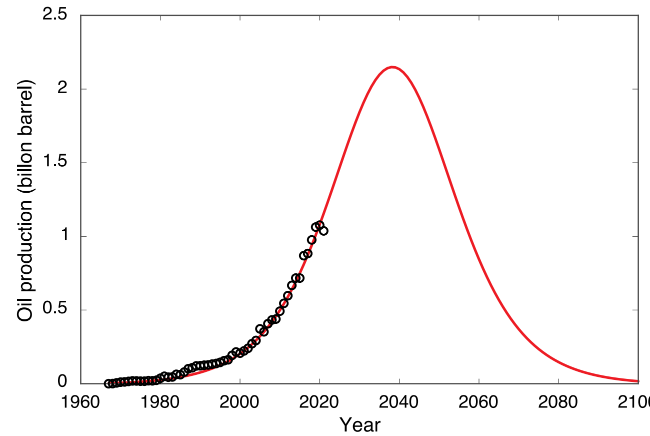

Fig. 2. We project future oil sands production in Alberta based on historical production data (black circles) using a logistic growth model (red line). The model predicts that production will peak in 2038.

2.3. Emission projection

We project oil sands production until the end of the century based on historical Alberta oil sands production data from 1967 to 2020 (CAPP, 2021) using a logistic growth model. Logistic growth models are often used to project the depletion of finite resources (e.g., hydrocarbons, groundwater), and they have been successfully applied to forecast the growth and decline of oil production (Hubbert, 1956; Clark et al., 2011; Sorrell and Speirs, 2019). Our model takes the form of

$$Q_{\mathrm{oil}} = \frac{\alpha \cdot V_{\mathrm{oil}} \cdot \exp(\alpha(t_{\mathrm{peak}} - t))}{\left(1 + \exp\left(\alpha(t_{\mathrm{peak}} - t)\right)\right)^2}, \tag{1}$$

where Q_{oil} is the annual oil production (1000 s m^3/year), V_{oil} is the total volume of recoverable oil (1000 s m^3), α is the growth rate (dimensionless), and t_{peak} is the time at which annual oil production peaks. We find that the logistic growth model perfectly fits the historical annual production data (Fig. 2). To project future CO_2 emissions associated with oil sands production, we calculate the amount

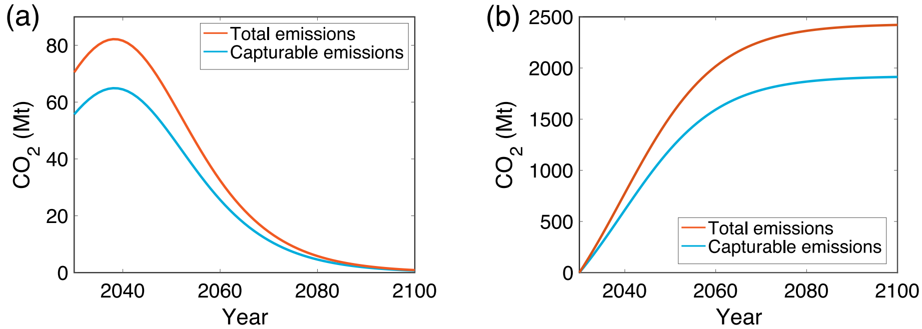

Fig. 3. (a) Projected annual total and capturable CO_2 emissions from the proposed CCS hub. (b) Projected cumulative total and capturable CO_2 emissions, given the CCS hub commences operation in 2030.

of CO_2 emissions per volume of oil produced based on 2019 emissions data (Government of Canada, 2021b), which yields an average oil sands CO_2 emissions intensity $I_{CO_2} = 0.449$ tonnes CO_2/m^3 oil produced. The projected annual total CO_2 emissions and capturable CO_2 emissions due to oil sands production in the proposed CCS hub are therefore given by $E_{\text{total}} = \beta I_{CO_2} Q_{\text{oil}}$ and $E_{\text{capture}} = RE_{\text{total}}$, where $\beta = 53\%$ is the ratio of CO_2 emissions from the CCS hub to the total oil sands emissions in Alberta, and $R = 79\%$ is the percentage of capturable emissions to total emissions. The annual capturable CO_2 emission from the CCS hub will reach a maximum level of 65 Mt in 2038 (Fig. 3a). Assuming that the CCS hub commences operation in 2030, the cumulative capturable CO_2 emissions will reach 1913 Mt by the end of the century (Fig. 3b).

3. Storage sites

The large amount of emissions associated with the CCS hub presents a tremendous opportunity and challenge for storage operations. To identify suitable storage formations, we apply the following criteria based on the relevant regulatory requirements and best practices: (i) The formation must be more than 1000 m deep to satisfy provincial guidelines on CO_2 injection (Alberta Energy Regulator, 2023); (ii) The formation must be thick and permeable to accommodate large amount of CO_2 (Bachu et al., 2014b; Burton et al., 2009); (iii) The formation must be geographically close to the CCS hub to minimize pipeline construction cost, as this is often a significant component of the overall cost of the CCS network and can make the difference between economic viability and unviability (Weihs and Wiley, 2012). We identify two thick and permeable aquifers, namely the Nisku and Wabamun formations, as ideal candidate storage sites. The areal footprints of each aquifer overlap each other, which further reduces the cost of pipeline construction since the same trunk line can service both aquifers.

The Nisku formation is a saline aquifer that terminates against the Precambrian Basement to the west (Alberta Geological Survey, 1994a) and rises towards the east at an average slope of 7 m/km in our study area (Bachu et al., 2014a). It is overlain by a thin layer of halite and the Calmar formation, and overlies a thin layer of shale and the Camrose and Grosmont formations (Bachu et al., 2014a). The Wabamun formation is a saline aquifer that also rises towards the east at an average rate of 7 m/km in our study area. It is overlain by the Banff formation and overlies the Winterburn group (Alberta Geological Survey, 1994a; Bachu et al., 2014a). Table 1 summarizes the aquifer properties associated with the Nisku and Wabamun formations. We use the geometric average of the maximum well-scale permeability across each aquifer (Bachu et al., 2014a).

In addition to aquifer properties, we characterize the properties of supercritical CO_2 and brine at aquifer conditions. The density of supercritical CO_2 is calculated using a correlation between density, pressure, and temperature based on the correlation method of Ouyang (2011). The dynamic viscosity of supercritical CO_2 is determined based on the correlation method introduced by Heidaryan et al. (2011). The density of brine is calculated based on the total dissolved solids (TDS) content of each aquifer and the density of water. The viscosity of brine as a function of pressure and temperature is calculated based on the empirical model developed by Klyukin et al. (2017). We assume that the dynamic viscosity of the dense mound μ_d is the same as that of the viscosity of brine for each aquifer. Table 2 summarizes the fluid properties associated with the Nisku and Wabamun formations.

Table 1
Aquifer properties of the Nisku and Wabamun formations, which include the aquifer thickness H, permeability k, porosity ϕ, slope S, injection well depth D, temperature T, pressure p, and bulk compressibility c (WorleyParsons, 2003; Szulczewski et al., 2012; Bachu et al., 2014a; Ghaderi and Leonenko, 2015; Alberta Geological Survey and Alberta Energy Regulator, 2021).

Formation	H [m]	k [mD]	ϕ [−]	S [−]	D [m]	T [K]	p [mPa]	c [GPa^{-1}]
Nisku	69	49.5	0.091	0.008	1960	338	19.3	0.4
Wabamun	183	42.7	0.128	0.007	1840	333	18.1	0.4

4. Pressure considerations

The injection of a large amount of CO_2 will inevitably increase aquifer pressure, and particular care must be taken to manage the pressure increase such that the maximum allowable limit is not exceeded. Exceeding the pressure limit could lead to the creation of new fractures, activation of existing faults, inducing seismicity, or enhancing pathways through which CO_2 could leak (Metz et al., 2005). Pressure buildup is a dynamic quantity that depends on the rate of CO_2 injection — aquifers that have sufficient pore spaces to accommodate the cumulative amount of intended CO_2 storage may not be able to sustain the required injection rate, which in our study is set by the projected annual capturable emissions (Fig. 3a). The storage capacity may thus be limited by the amount of CO_2 that can be injected over time without exceeding the fracture pressure or maximum permitted pressure of the aquifer, which is defined as the pressure-limited storage capacity (Bachu, 2015; Szulczewski et al., 2012).

The evolution of pressure in the aquifer over time must be modelled to determine the storage capacity. Bachu (2016) notes that the injection pressure should be less than the minimum stress pressure (rather than the formation fracture pressure) to avoid opening existing fractures in the formation. We use a minimum horizontal stress gradient value of 20 kPa/m as the formation pressure limit, which was reported for the Nisku formation by Goodarzi et al. (2012) and Bell and Bachu (2003). We assume that this value is also applicable to the Wabamun formation since the Nisku underlays the Wabamun at this point and both are comprised of carbonate rocks (Bachu et al., 2014a). The maximum injection pressure is determined according to provincial regulations that limit the maximum borehole pressure to 90% of the formation pressure limit (AER, 1994), which gives 35.3 MPa and 33.1 MPa as the pressure limits for Nisku and Wabamun respectively.

Table 2
Fluid properties in the Nisku and Wabamun formations, which include brine density ρ_w, CO_2-saturated brine density ρ_d, supercritical CO_2 density ρ_g, brine viscosity μ_w, supercritical CO_2 viscosity μ_g, and salinity σ (Bachu et al., 2014a; Ouyang, 2011; Heidaryan et al., 2011).

Formation	ρ_w [kg/m^3]	ρ_d [kg/m^3]	ρ_g [kg/m^3]	μ_w [Pa s]	μ_d [Pa s]	μ_g [Pa s]	σ [mg/L]
Nisku	1180	1188	675	6.33×10^{-4}	6.33×10^{-4}	5.25×10^{-5}	180 000
Wabamun	1170	1178	686	6.70×10^{-4}	6.70×10^{-4}	5.32×10^{-5}	170 000

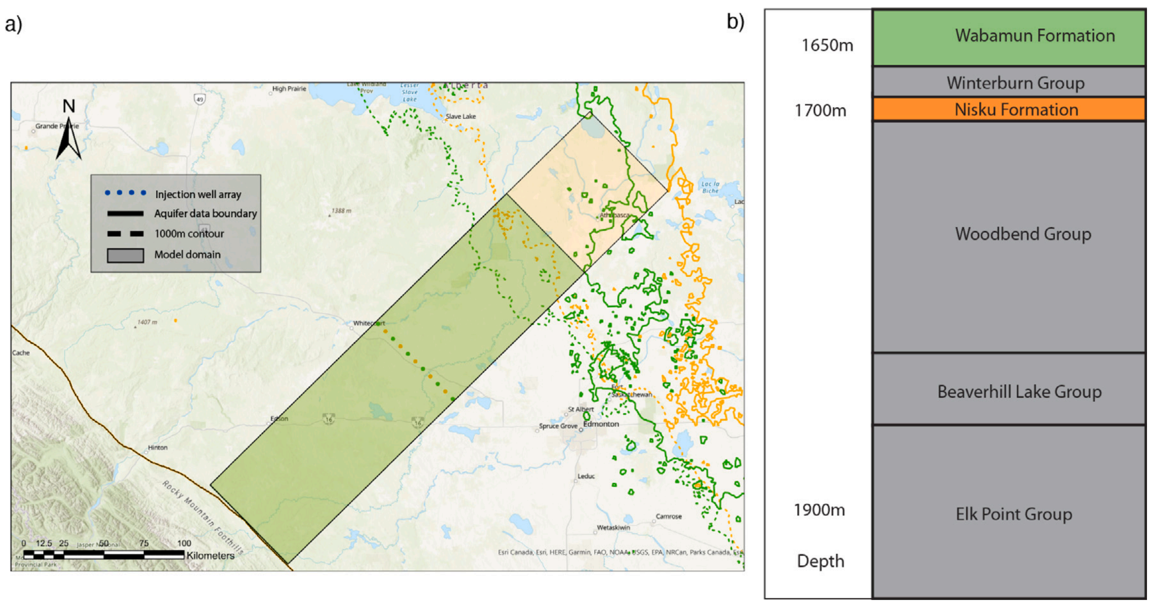

Fig. 4. (a) The pressure and migration model domains of Wabamun (green) and Nisku (orange) aquifers. The solid lines represent the aquifer boundary while the dashed lines represent the 1000-m depth contour line. The circles in the middle of the domains represent the injection well array, with wells injecting alternatively into each aquifer. (b) The depths of the Nisku and Wabamun formations in relation to other formations in our study area.

Since CO_2 is injected along a line-drive well array with closely-spaced individual wells, we can collapse the dimension along the line drive and use a simple 1D model to predict pressure evolution in the dimension perpendicular to the line drive (Nicot, 2008; Szulczewski et al., 2014). The model is a partial differential equation based on conservation of volume and Darcy's law, and it is of the form (Pinder and Gray, 2008; Szulczewski et al., 2014):

$$c\frac{\partial p}{\partial t} - \frac{k}{\mu_w}\frac{\partial^2 p}{\partial x^2} = \frac{Q}{HW}, \quad (2)$$

where c is the bulk compressibility, p is the fluid pressure, k is the aquifer's absolute permeability, μ_w is the viscosity of brine, x is the lateral coordinate, Q is the volumetric injection rate of CO_2, H is the aquifer thickness, and W is the width of the injection well array. The assumptions associated with this simple pressure model has been extensively discussed in Szulczewski et al. (2014). Here, we note two assumptions that warrant particular attention: (i) the model assumes the compressibility of CO_2 at aquifer conditions to equal that of the ambient brine, which will result in an overestimation of pressure increase due to CO_2 injection. Therefore, the model will provide a conservative estimate of maximum viable CO_2 injection rates; (ii) the model assumes uniform pressure along the well array (i.e., linear flow), which could lead to an underestimation of pressure increase. This assumption is valid if pressure equilibration between individual wells is relatively quick compared to the total injection duration. The timescale of pressure equilibration t_{eq} can be approximated by (Szulczewski et al., 2012)

$$t_{eq} = \frac{l^2 c \mu_d}{k}, \quad (3)$$

where l is the distance between individual wells. We set the well spacing to be $l = 2$ km, which gives $t_{eq} = 0.7$ years. Therefore, the assumption of uniform pressure along the array is valid since t_{eq} is approximately 1% of the total injection duration.

Our model domain is oriented such that the left boundary is west and the right boundary is east (Fig. 4a). A stratigraphic cross-section of the Nisku formation shows that it onlaps onto a dolomite formation, possibly the Duvernay, which then terminates against the Peace River Arch (Alberta Geological Survey, 1994a). We assume a no-flow boundary condition here. The Wabamun formation experiences a discontinuity as a result of a fault at the western edge of our model domain, which also indicates a no-flow boundary condition for the left boundary (Alberta Geological Survey, 1994b). The right (east) boundaries of both formations reach sea level in our model domain (Bachu et al., 2014a), thus we assume atmospheric pressure here. Finally, we assume the initial pressure in the aquifers to be hydrostatic. We solve Eq. (2) numerically using a finite difference method and fourth-order Runge–Kutta time-stepping.

For a given aquifer, the amount of pressure increase is controlled by the CO_2 injection flux $q = Q/(HW)$. Pressure increase can therefore be modulated by adjusting the volumetric injection rate Q and the length of the well array W. We apportion the total projected annual capturable emissions (Fig. 3a) between Nisku and Wabamun and solve Eq. (2) iteratively to obtain the minimum W that satisfy the maximum allowable pressure limit throughout the entire project duration. Our modelling results suggest a 70%/30% apportionment of the total projected annual capturable emissions between Wabamun and Nisku, and $W = 65$ km will accommodate the entire 1.91 Gt of capturable emissions while satisfying the pressure limit. Under this configuration, the maximum pressure in each aquifer is reached in 2053, approximately 24 years after the start of injection. Specifically, Wabamun reaches a maximum pressure of 32.3 MPa while Nisku reaches a maximum pressure of 34.1 MPa (Fig. 5).

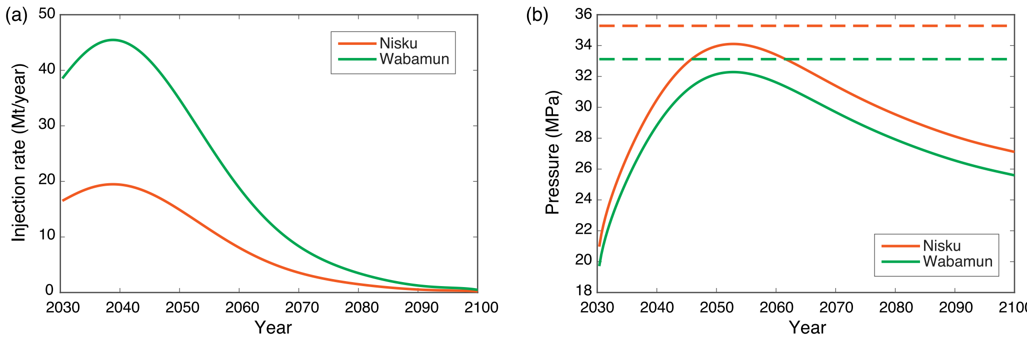

Fig. 5. (a) Annual CO_2 injection rates in the Nisku (orange) and Wabamun (green) formation. The injection rate in each aquifer peaks in 2038 with the projected peak in oil sands emissions (Fig. 3) and declines thereafter. (b) Aquifer pressure evolution (solid lines) and local maximum pressure limits (dashed lines) in the Nisku (orange) and Wabamun (green) formations. Aquifer pressures are projected to peak in 2053 before declining for the remainder of the injection period.

5. Migration considerations

The injected CO_2 is less dense than the ambient brine and it will migrate upward due to buoyancy and spread along the caprock as a gravity current. In the absence of trapping, the CO_2 gravity current will spread indefinitely. This is undesirable since the CO_2 could encounter potential leakage pathways such as faults or abandoned wells. Fortunately, trapping mechanisms exist to immobilize the CO_2 and limit its migration distance. Well-known trapping mechanisms include residual trapping, where tiny blobs of CO_2 are immobilized by capillary forces at the pore-scale, and solubility trapping, where CO_2 dissolves into the ambient brine and sink to the bottom of the aquifer (Hesse et al., 2008; MacMinn et al., 2011). In the context of CO_2 storage in the Nisku and Wabamun formations, the lateral migration of the CO_2 gravity current could take it above the 1000 m depth threshold beyond which CO_2 storage is prohibited as per the provincial guideline. Therefore, it is important that the injected CO_2 be completely immobilized before reaching the 1000 m below the ground surface contour line (Fig. 4).

Here, we simulate the evolution of the CO_2 gravity current using a 1D sharp interface model. Sharp interface models are able to simulate flow over large distances due to their low computational cost compared to full numerical simulations (Bandilla et al., 2019), and they can be formulated to include residual trapping and solubility trapping (Hidalgo et al., 2013). Our model consists of two coupled partial differential equations that describe the evolution of the buoyant CO_2 current and the mound of brine saturated with dissolved CO_2 (hereafter referred to as the dense mound). In its dimensionless form, the model is expressed as:

$$\frac{\partial \tilde{h}_g}{\partial \tilde{t}} + \frac{1}{(1-S_{wc}-S_{gr}\tilde{R})}\frac{\partial}{\partial \tilde{x}}\left[\delta(1-\tilde{f}_g)\tilde{h}_g(\sin\theta - \cos\theta\frac{\partial \tilde{h}_g}{\partial \tilde{x}}) + \tilde{f}_g\tilde{h}_d(\sin\theta+\cos\theta\frac{\partial \tilde{h}_d}{\partial \tilde{x}})\right] = -N_d, \tag{4a}$$

$$\frac{\partial \tilde{h}_d}{\partial \tilde{t}} - \frac{\partial}{\partial \tilde{x}}\left[\delta\tilde{f}_d\tilde{h}_g(\sin\theta - \cos\theta\frac{\partial \tilde{h}_g}{\partial \tilde{x}}) + (1-\tilde{f}_d)\tilde{h}_d(\sin\theta+\cos\theta\frac{\partial \tilde{h}_d}{\partial \tilde{x}})\right] = \frac{N_d}{\chi_v}(1-S_{wc}-S_{gr}\tilde{R}), \tag{4b}$$

where $\tilde{h}_g = h_g/H$ and $\tilde{h}_d = h_d/H$ are the local dimensionless thickness of the CO_2 current and the thickness of the dense mound, respectively. $\tilde{x} = x/H$ is the dimensionless lateral coordinate and θ is the aquifer slope. S_{wc} is the connate water saturation, which accounts for the fraction of pore spaces occupied by immobile brine in the wake of CO_2. Similarly, S_{gr} is the residual gas saturation, which represents the fraction of pore spaces occupied by blobs of trapped CO_2. We assume $S_{wc} = 0.3$, $S_{gr} = 0.3$ for both Nisku and Wabamun formations, based on relative permeability curves of the Nisku carbonate measured at reservoir conditions (Bennion and Bachu, 2008). The discontinuous coefficient $\tilde{R}$ accounts for the fact that residual trapping only occurs in areas where the CO_2 gravity current has been displaced by brine. Specifically, $\tilde{R} = 1$ if $\partial\tilde{h}_g/\partial\tilde{t} < 0$, and $\tilde{R} = 0$ if $\partial\tilde{h}_g/\partial\tilde{t} \geq 0$. $\tilde{f}_g$ and $\tilde{f}_d$ are the dimensionless fractional flow functions:

$$\tilde{f}_g = \frac{\tilde{h}_g M_g}{\tilde{h}_g(M_{gw}-1)+\tilde{h}_d(M_{dw}-1)+1}, \tag{5a}$$

$$\tilde{f}_d = \frac{\tilde{h}_d M_d}{\tilde{h}_g(M_{gw}-1)+\tilde{h}_d(M_{dw}-1)+1}, \tag{5b}$$

$$M_{gw} = \frac{\lambda_g}{\lambda_w}, \tag{5c}$$

$$M_{dw} = \frac{\lambda_d}{\lambda_w}, \tag{5d}$$

where $\lambda_g = kk_{gr}/\mu_g$, $\lambda_w = k/\mu_w$, and $\lambda_d = k/\mu_d$ are the mobilities of the CO_2 current, ambient brine, and dense mound respectively. μ_g, μ_w, μ_d are the dynamic viscosities of the respective fluid phases, and $k_{gr} = 0.55$ is the measured end-point relative permeability of CO_2 (Bennion and Bachu, 2008). Here, we assume the dynamic viscosities of the ambient brine and the dense mound equal each other, such that $M_{dw} = 1$, and Eq. (4) contains dimensionless time $\tilde{t} = t/T_c$, and the characteristic time T_c is given by:

$$T_c = \frac{H\phi}{\lambda_d \Delta\rho_{dw} g}, \tag{6}$$

where $\Delta\rho_{dw}$ is the density difference between the dense mound and ambient brine. Finally, Eq. (4) contains two additional dimensionless parameters δ and N_d, which are given by:

$$\delta = \frac{\lambda_g \Delta\rho_{gw}}{\lambda_d \Delta\rho_{dw}}, \tag{7a}$$

$$N_d = \frac{q_d}{\lambda_d \Delta\rho_{dw} g\phi}, \tag{7b}$$

where $\Delta\rho_{gw}$ is the density difference between the buoyant CO_2 and the ambient brine. $q_d = \varphi\chi_v\phi\Delta\rho_{dw}g\lambda_d$ is the volumetric rate of convective dissolution per unit area of fluid–fluid interface (Szulczewski et al., 2012), where φ is a constant roughly equal to 0.01 (Pau et al., 2010) and $\chi_v = 0.052$ is the solubility of CO_2 in brine, expressed as the volume of free-phase CO_2 that can be dissolved per unit volume of brine saturated with CO_2.

The initial condition for the migration model corresponds to the shape of the CO_2 plume at the end of the injection period, and it is given by (Nordbotten et al., 2005; Juanes et al., 2010):

$$\tilde{h}_g = \frac{\sqrt{\frac{M_{gw}}{\tilde{x}/\tilde{I}}}-1}{M_{gw}-1}, \tag{8a}$$

$$\tilde{I} = \frac{V_{CO_2}}{\phi W H^2}, \tag{8b}$$

where V_{CO_2} is the total volume of injected CO_2. According to our simulations, the stored CO_2 in Wabamun aquifer will be completely

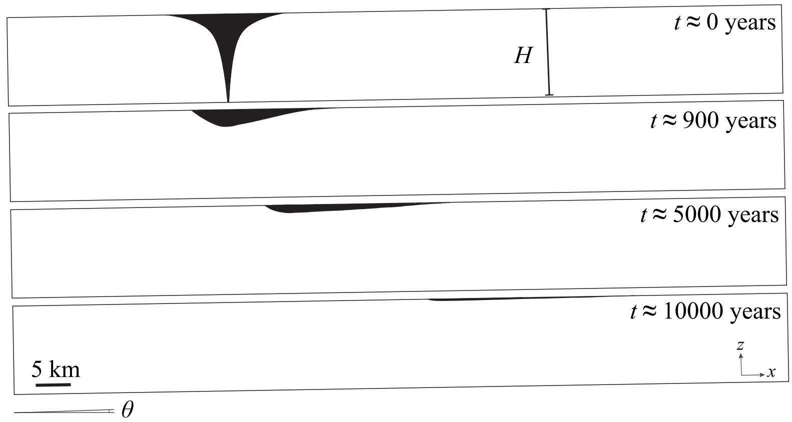

Fig. 6. Simulation of the CO_2 plume profile at Wabamun aquifer after the injection period ends. The volume of mobile CO_2 decreases due to residual trapping and solubility trapping. Note that the vertical scale of the aquifer is greatly exaggerated in the figure.

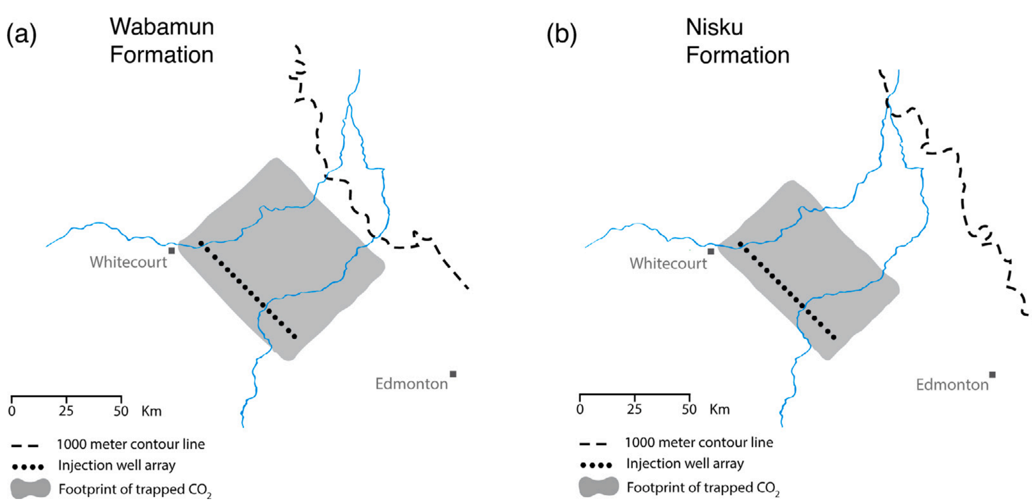

Fig. 7. (a) The ultimate CO_2 footprint in the Wabamun formation, which illustrates the areas invaded by the free-phase CO_2 before it becomes completely trapped. (b) The ultimate CO_2 footprint in the Nisku formation.

immobilized by residual trapping and solubility trapping after about 11000 years. During that time, the CO_2 plume will have migrated approximately 55 km to the right and 9 km to the left of the well array (Fig. 7a). The same goes for injected CO_2 in Nisku aquifer, which will be completely immobilized after about 6900 years, during which time it will have travelled approximately 40 km to the right and 9 km to the left of the well array (Fig. 7b). In both cases, the injected CO_2 will be fully immobilized before reaching the 1000 m depth contour line of the aquifers.

6. Uncertainty considerations

The use of simple 1D models to simulate pressure increase and CO_2 migration is driven by the lack of certainty and spatial coverage of relevant hydrogeologic data in the study area, which makes it infeasible to apply three-dimensional (3D) computational models. Here, we estimate the range of the pressure and migration-limited storage capacities due to uncertainties in the input parameters. The pressure-limited capacity is defined as the maximum storage capacity of an aquifer without surpassing 90% of the formation pressure limit at the injection wells, while the migration-limited capacity is defined as the maximum amount of CO_2 an aquifer can trap before the mobile plume reaches the aquifer's 1000 m depth contour line. Specifically, we consider permeability, rock compressibility, and aquifer thickness as the uncertain parameters in the pressure model (Ranaee et al., 2022). For the migration model, we consider relative gas permeability, residual gas saturation, connate water saturation, porosity, permeability, and aquifer thickness as the uncertain parameters. We utilize one of three methods to estimate either the maximum or minimum value of each uncertain input parameter, which is then combined to yield the most conservative storage capacity estimate. Based on the sensitivity analysis performed for similar pressure and migration models by Szulczewski et al. (2012), the pressure-limited capacity decreases as the permeability, rock compressibility, and aquifer thickness decrease. Therefore, we need the minima of these parameters to estimate the minimum pressure-limited capacity. Meanwhile, the migration-limited capacity decreases as the porosity, aquifer thickness, residual gas saturation decrease and connate water saturation increases. We adopt this simple extrema method for uncertainty quantification due to the lack of probability density functions for the parameters of interest. Bachu et al. (2014a) provided heat maps depicting porosity and aquifer thickness distribution of Wabamun and Nisku formations, which enables us to directly obtain the minimum porosity and thickness values within the model domains (Tables 4 and 3). Due to lack of data, we estimate an absolute parameter uncertainty $\Delta\mathcal{P}$ and apply it equally in both directions around the parameter mean $\mathcal{P}_0$ to find the minimum or maximum values of residual gas saturation, relative gas permeability, and connate water saturation (Tables 4 and 3) (Szulczewski et al., 2012). Porosity, bulk compressibility, and permeability are often considered log-normally distributed, so we estimate a relative uncertainty ψ in the log form of the parameter (in SI units), such that the minimum of these

Table 3
Extrema values of the parameters used to obtain the conservative estimates of pressure- and migration-limited capacities for the Wabamun formation.

Parameter	Symbol	Mean	Min	Max	Method	$\Delta\mathcal{P}$	Ψ
Permeability [mD]	k	42.7	26.9	–	Relative uncertainty	–	0.03
Bulk compressibility [GPa^{-1}]	c	0.4	0.29	–	Relative uncertainty	–	0.03
Porosity [–]	ϕ	0.128	0.05	–	Direct reading	–	–
Aquifer thickness [m]	H	183	175	–	Direct reading	–	–
Residual gas saturation [–]	S_{gr}	0.1	0.05	–	Absolute uncertainty	0.05	–
Relative gas permeability [–]	k_{gr}	0.55	–	0.65	Absolute uncertainty	0.1	–
Connate water saturation [–]	S_{wc}	0.2	–	0.3	Absolute uncertainty	0.1	–

Table 4
Extrema values of the parameters used to obtain the conservative estimates of pressure- and migration-limited capacities for the Nisku formation.

Parameter	Symbol	Mean	Min	Max	Method	$\Delta\mathcal{P}$	Ψ
Permeability [mD]	k	49.5	31.2	–	Relative uncertainty	–	0.03
Bulk compressibility [GPa^{-1}]	c	0.4	0.29	–	Relative uncertainty	–	0.03
Porosity [–]	ϕ	0.091	0.05	–	Direct reading	–	–
Aquifer thickness [m]	H	69	25	–	Direct reading	–	–
Residual gas saturation [–]	S_{gr}	0.1	0.05	–	Absolute uncertainty	0.05	–
Relative gas permeability [–]	k_{gr}	0.55	–	0.65	Absolute uncertainty	0.1	–
Connate water saturation [–]	S_{wc}	0.2	–	0.3	Absolute uncertainty	0.1	–

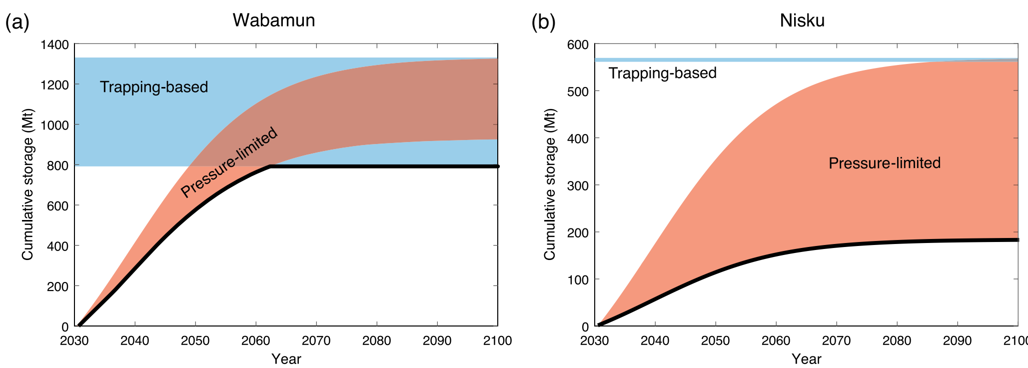

Fig. 8. The range of pressure- and migration-limited storage capacity for (a) Wabamun and (b) Nisku formations obtained using the extrema method for uncertainty quantification. The range of storage capacities is bounded at the top by the average value of the input parameters and at the bottom by parameter values that yield the most conservative estimate. The solid line indicates the cumulative storage capacity evolution under this worst-case scenario.

parameters are given by $\mathcal{P}_{\min} = \mathcal{P}_0^{(1+\psi/2)}$ (Tables 3 and 4) (Szulczewski et al., 2012).

The extrema method reveals that the injection rate at Wabamun will be limited by formation pressure increase in the first half of its operation lifetime, and then it will be limited by CO_2 migration. The worst-case scenario considered here yields a storage capacity of 0.82 Gt compared to the baseline capacity of 1.34 Gt for Wabamun (Fig. 8a). Meanwhile, the injection rate at Nisku will be limited by formation pressure increase alone, and the worst-case scenario storage capacity is 0.19 Gt compared to the baseline capacity of 0.57 Gt (Fig. 8a). The combined worst-case scenario storage capacity is 1 Gt compared to the baseline capacity of 1.91 Gt.

7. Pipeline design

The collection and transport of the captured CO_2 from the CCS hub to the storage sites require an extensive network of pipelines. We design the pipeline network following a trunk-and-branch model, where each emitter is connected to the large trunk line by smaller branch lines. The trunk-and-branch model has been shown to yield reduced cost and shorter overall network length compared to the traditional point-to-point model (Kuby et al., 2011; Peletiri et al., 2018). Additionally, we follow the rights-of-way of existing oil and gas pipelines to ensure that our network does not intrude sensitive regions (e.g., provincial or national parks, conservation areas, etc.) and is built on land suitable for pipeline construction and operation. In the trunk-and-branch model the most efficient network is defined as the one with the shortest total length. We manually edit the potential network configurations given by the existing rights-of-way until we achieve the most efficient network (Fig. 9) (Edwards and Celia, 2018).

We determine the size of each pipeline segment based on the maximum expected mass flow rate during the project duration using the modified Darcy–Weisbach equation (Eq. (9)) (McCollum and Ogden, 2006)

$$D_{\mathrm{p}} = \left(\frac{32 f_f q_{\max}^2 L}{\pi^2 \rho_{CO_2} \Delta P_L}\right)^{0.2}, \tag{9}$$

where D_{p} [m] is the inner diameter of pipeline, $q_{\max}$ [kg/s] is the maximum mass flow rate, f_f [–] is the Fanning friction factor, ρ_{CO_2} [kg/m^3] is the density of CO_2, ΔP_L [Pa] is the pressure loss along the pipeline segment, and L [m] is the length of the pipeline segment. The maximum mass flow rate in each pipeline segment corresponds to the sum of all upstream flow during the year of peak CO_2 production illustrated in Fig. 5a. Our pressure and migration models show that this maximum injection rate is physically feasible, though uncertainties in the hydrogeologic parameters could significant lower the maximum injection rate. The trunk line inlet and outlet pressures are set to 2100 psi and 1400 psi respectively, which are typical compressor outflow pressures and oilfield delivery pressures (Edwards and Celia, 2018). The branch line outlet pressures are set to 2100 psi to match the inlet pressure of the trunk line. We have assumed the pipelines to be manufactured using carbon steel due to its superior strength, durability, and corrosion resistance (McCollum and Ogden, 2006; McCoy and Rubin, 2008). The resulting pipeline diameters are shown in Table 5.

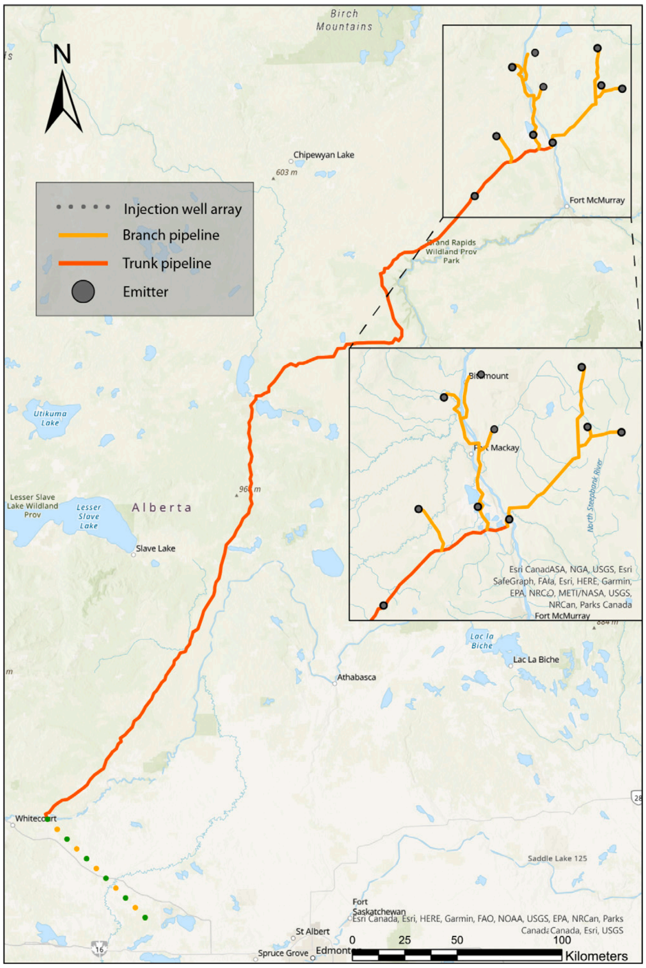

Fig. 9. The pipeline network consists of a high-capacity trunk line (red line) connecting each emitter (grey dots) in the CCS hub to the injection well array (dotted line) via smaller branch lines (orange lines).

8. Economic considerations

Our proposed CCUS system is a large-scale infrastructure project that requires significant capital and operational expenditure associated with retrofitting existing facilities to enable carbon capture, as well as constructing the pipeline network to enable CO_2 transport. The CO_2 capture cost is facility-dependent, since it is a function of the specific capture technology used and the purity of the CO_2 stream, with the cost per tonne decreasing as the CO_2 concentration in the captured gas increases. Since the equipment used in CO_2 capture will be installed at and used by each emitter, we assume that the capital and operational cost associated with CO_2 capture will be borne by each emitter.

The capital expenditure of the pipeline network is likely to be the largest contributor to the overall capital expenditure of the CCUS system (Edwards and Celia, 2018) and is thus the focus. The costs presented in Sections 8.1–8.3 are in 2025 Canadian dollars (CAD), which we assume to be the first year of construction. When necessary, we use data from the U.S. Bureau of Labor Statistics (2022) to adjust figures originally presented in U.S. dollars (USD) to adjust for inflation and take the average USD to CAD conversion rate over the past five years from the Bank of Canada (2022) to convert to 2023 CAD. We then use the Bank of Canada's target inflation rate to escalate from 2023 CAD to 2025 CAD (Bank of Canada, 2016).

8.1. Pipeline cost

We use the NETL CO_2 Transport Cost Model (National Energy Technology Laboratory, 2018) to estimate the capital cost for constructing the pipeline network. Specifically, the model calculates the capital cost as

$$C = \alpha_{i-0} + L(\alpha_{i-1} D_\text{p}^2 + \alpha_{i-2} D_\text{p} + \alpha_{i-3}), \tag{10}$$

where C is the capital cost, L is the pipeline length, D_p is the pipeline diameter, and $\alpha_{i-1}, \alpha_{i-2}, \alpha_{i-3}$ are empirical cost parameters determined by fitting the equation to existing pipeline capital cost data (Parker, 2004; National Energy Technology Laboratory, 2018). The empirical cost parameters are functions of various engineering inputs. Specifically, we use the model default of 15% for the contingency factor, which covers miscellaneous costs. We assume that construction will start in 2025 and complete in 2029. Table 5 summarizes the cost of each pipeline segment. The total capital cost of the pipeline network is \$ 3.97-billion, which includes the costs of the branch lines, the trunk line, and a pipeline that connects each injection well to the trunk line. The capital cost for each pipeline segment includes the cost of materials, labor, rights of way, damages, CO_2 surge tanks, pipeline control system, and pumps.

8.2. Injection well cost

We assume CO_2 will be injected into Nisku and Wabamun formations along a 65 km-long linear well array (Fig. 9). Since the Wabamun formation overlaps the Nisku formation (Fig. 4b), we design an overlapping injection well array such that only one pipeline is required to connect each injection well. In this design the injection wells are spaced 1 km apart and alternately inject into Nisku and Wabamun formations. Our injection array requires the construction of 67 individual injection wells. Nygaard and Lavoie (2009) estimated the capital cost of drilling and completing a vertical injection well in the Nisku formation to be \$ 1.19-million in 2009, which is equivalent to \$ 1.69-million when adjusted for inflation. We assume that the cost of drilling and completing an injection well in the Wabamun formation to be the same, which is a conservative assumption since the Wabamun formation is shallower than the Nisku formation. Therefore, the total capital cost of constructing the injection wells is \$ 113.4-million. The total capital cost of the pipeline network and the injection well array adds up to \$ 4.09-billion in 2025.

8.3. Cost comparison

The cost per inch of diameter per km of length is a commonly-used metric that normalizes the cost of pipelines of different sizes and lengths. Smith et al. (2021) identified the range of capital costs for onshore CO_2 pipelines in 2019 USD/in/mile from three sources, which we adjust for inflation and convert to 2025 CAD/in/km (Table 6). Our proposed pipeline network's capital cost is \$ 143,580/in/km, which is higher than the ranges of Heddle et al. (2003) and the National Energy Technology Laboratory (2018) but within the range presented by the National Petroleum Council (NPC, 2019). Comparing our estimated cost to the capital cost of an existing CO_2 pipeline in Alberta lends additional context. The ACTL, a 240 km pipeline, has an estimated capital cost of \$ 397,262/in/km (Cole and Itani, 2013).

8.4. Financial and policy incentives

One of the biggest obstacles to the implementation of large-scale CCUS projects is the lack of reliable funding to offset the high capital cost (Boot-Handford et al., 2014; Alcalde et al., 2019; Budinis et al., 2018; Ciotta et al., 2021). Fortunately, the Government of Canada has recently introduced several financial incentives that will significantly

Table 5
Key parameters and capital costs of each pipeline segment and the injection array. The capacity of each segment is equivalent to the peak upstream CO_2 flow.

Pipeline segment type	Capital cost (2025 CAD)	Capacity (Mt/yr)	Diameter (in)	Length (km)
Branch lines	$41.1M	4.68	16	24
	$7.9M	2.88	16	2
	$18.0M	9.07	16	9
	$11.9M	11.95	16	5
	$71.6M	16.62	20	34
	$11.3M	29.53	24	3
	$19.5M	3.65	12	14
	$21.2M	8.31	16	11
	$23.8M	11.96	16	13
	$13.2M	2.53	12	8
	$30.5M	14.49	16	17
	$7.2M	19.32	20	2
	$20.2M	33.81	20	8
	$17.3M	0.67	8	15
Trunk line	$3290.1M	64.90	48	467
Injection array pipeline	$371.2M	64.90	42	66
Pipeline cost	$3976.7M			
Injection wells	$113.4M			
Total capital cost	**$4090.1M**			

Table 6
Range of onshore CO_2 pipeline cost per inch of diameter per km of length (Smith et al., 2021).

Capital cost range (2025 CAD/in/km)			
Low	Mean	High	Source
$17,469	$50,781	$84,093	Heddle et al. (2003)
$38,454	$49,523	$80,533	National Energy Technology Laboratory (2018)
$76,807	$110,411	$144,014	NPC (2019)

benefit the proposed CCS hub and help offset the capital and operational costs associated with CCUS activities. Specifically, the Net Zero Accelerator (NZA) initiative will provide up to $8-billion to support projects that reduce Canadian GHG emissions (Government of Canada, 2021c). A key targeted area for support under the NZA initiative is the decarbonization of large emitters (Government of Canada, 2021d), which is in perfect alignment with the proposed CCS hub. In addition to direct funding support, the Government of Canada proposed an investment tax credit for Carbon Capture, Utilization, and Storage (the CCUS Tax Credit) for projects that sequester more than 15 Mt annually (Government of Canada, 2021a), which was reaffirmed in the most recent climate action plan (Environment and Climate Change Canada, 2022). The draft legislative proposal sets out a tax credit of 50% of eligible expenditures related to acquiring CO_2 capture equipment between 2022–2030 and 25% between 2031–2040 (Department of Finance Canada, 2022). Eligible expenditures related to acquiring CO_2 transportation and storage equipment can also generate tax credits at 37.5% between 2022–2030 and 18.75% between 2031–2040 (Department of Finance Canada, 2022). Emitters participating in the CCS hub will directly benefit from the tax credit.

In addition to financial incentives, a hospitable policy environment is equally important to spur the creation of large scale CCUS projects (Bäckstrand et al., 2011; Yao et al., 2018; Budinis et al., 2018; Alcalde et al., 2019; Romasheva and Ilinova, 2019). On the policy front, the federal government recently established the Clean Fuel Regulation which requires a reduction in the carbon intensity of liquid fuels produced and sold in Canada (Department of the Environment, 2020; Government of Canada, 2022). This regulation directly applies to primary suppliers of liquid fuel, defined as entities who operate a facility at which gasoline or diesel is produced, rather than upstream facilities such as the oil sands bitumen extractors included in our study which produce crude oil. However, upstream facilities are still incentivized to reduce the carbon intensity of the fuels they produce due to the opportunity to create credits which can be sold to primary suppliers and other parties to the regulation. CCUS is an attractive method to reduce the carbon intensity of fuels and is noted as such by the government (Government of Canada, 2022). Additionally, the federal government reaffirmed its commitment to further CCS deployment by eliminating regulatory barriers and increasing coordination between the public and private sectors, and it identified Alberta and Saskatchewan as potential CCUS hubs (Government of Canada, 2021a; Environment and Climate Change Canada, 2022).

On the provincial level, the Alberta government recently increased the provincial carbon price payable under the TIER regulation to remain consistent with the federal carbon pricing benchmark, rising to $170/tonne by 2030 (Potkins, 2022). The government also created a sequestration credit for companies utilizing CCUS technology, with each credit offsetting one tonne of CO_2 emitted into the atmosphere (Potkins, 2022). This change increases the incentive for emitters to participate in a CCS hub by both increasing the financial penalty for emitting CO_2 and enabling participating emitters to create direct value via the generation of sequestration credits, which can be used to offset non-capturable emissions. Our proposed system will take advantage of the support offered by the favourable policy environment on the federal and provincial levels to reduce emissions and create a pathway towards net zero emissions.

While the Canadian government has already established some financial and policy incentives to support CCUS projects, additional incentives could help further accelerate the creation of large CCUS hubs at the scale proposed here. These incentives would not only help Canada reach its emission reduction target but also benefit the provincial and federal economies, since building a CCUS hub at this scale will require the creation of many jobs and participation of all levels of government.

8.5. Economic analysis

We investigate the economic viability of the construction of the proposed pipeline network by a private consortium, taking advantage of the federal CCUS Tax Credit (Government of Canada, 2021a). Specifically, the CCUS Tax Credit would be provided at a rate of 37.5% for the cost of purchasing and installing eligible CCUS equipment incurred between 2022 to 2030. Additionally, transportation equipment (i.e., pipelines) and storage equipment (i.e., injection wells) are included in the capital cost allowance (CCA) class with a declining balance rate of 8%. We assume 100% of the financing for the proposed pipeline will come from equity (i.e., no cost of debt), and that the capital expenses (CAPEX) will be evenly distributed during pipeline construction (i.e.,2025–2029). Once the pipeline becomes operational in 2030, the pipeline owner will generate revenue by charging a tariff per ton of CO_2 transported, which will be escalated at a rate of 3% each year. The pipeline owner will incur operations and maintenance expenses (OPEX), which are calculated using the NETL CO_2 Transport Cost Model (National Energy Technology Laboratory, 2018) and inflation adjusted at 3% each year. In our economic model, tax is levied against earnings of the pipeline operations, which is given by revenue minus the sum of depreciation and OPEX. We apply a corporate tax rate of 23%, which includes 15% federal tax and 8% provincial tax for Alberta. Finally, we calculate the tariff that the pipeline owner need to charge to achieve a target internal rate of return (IRR) of 8% over a specific period. The resulting tariffs are $ 7.09/tonne over a 50-year period and $ 8.13/tonne over a 20-year period, both tariffs are given in 2030 dollar value. The spreadsheet for the economic analysis is provided in *SI Appendix*.

An alternative to the construction of the pipeline network by a private consortium is for the federal or provincial government to finance the project completely. Federal infrastructure spending has risen over the past five years and is projected to continue to rise over the next six years. The Parliamentary Budget Officer (2022) projects that the federal government will spend $ 32.3-billion on infrastructure in the 2026–2027 fiscal year, up from $ 22.8-billion in the 2020–2021 fiscal year. This is much greater than the total capital cost of the proposed pipeline system. In addition, the total cost would be spread over the length of the construction period, further reducing the demand on federal infrastructure spending each year. It is thus conceivable for the government to fund and own the transport pipeline in its entirety. There are precedents of the federal government investing in large-scale infrastructure projects to tackle the problem of the day, such as investments of nearly $ 2-billion dollars each in the GO Transit Expansion Project and the Ontario Line (Infrastructure Canada, 2016). Other large-scale investments include the extension of the Montreal Metro and the Scarborough Subway (Infrastructure Canada, 2016). Altogether, there have been six projects with investments of greater than $ 1-billion each since 2002 (Infrastructure Canada, 2016). The Government of Canada has invested over $ 129-billion since 2016 through the Investing in Canada Plan and has committed to investing an additional $ 51 billion over the next five years (Infrastructure Canada, 2022). It is clear that the federal government has a history of investing in large-scale infrastructure projects and intends to continue this investment.

9. Conclusion

This paper proposes the establishment of a gigaton-scale CCS hub that captures CO_2 from a dense cluster of 10 emitters in the Athabasca oil sands region and transports it to deep saline aquifers for permanent storage (Fig. 1). We take a holistic approach in evaluating the feasibility of the CCS hub, which includes considering future emissions projections, emission capture and transport, pressure and migration capacity of the storage aquifers, the costs and financing required, as well as the regulatory and policy environment. Specifically, we project the future capturable annual emissions of the cluster using a logistic growth model, which adds up to over 1.9 Gt for the remainder of the century (Figs. 2–3). We identify the Nisku and Wabamun formations as ideal storage sites for the captured CO_2 (Fig. 4). Using the capturable emissions projections as the injection schedule, we model the aquifer pressure evolution during injection (Fig. 5) and CO_2 plume migration post-injection to ensure the storage operations satisfy all regulatory requirement (Figs. 6–7). The models, though extremely simplified, provide physical bounds on the pressure- and migration-limited storage capacities and they show that the Nisku and Wabamun formations can accommodate all of the captured emissions based on average aquifer properties. However, uncertainties in relevant aquifer properties could significantly reduce the storage capacity (Fig. 8). To connect the emitters and the storage formations, we design a trunk-and-branch pipeline network that minimizes the total pipeline length (Fig. 9). The construction of the pipeline network represents the majority of the capital expenditure associated with the CCS hub, which we estimate to cost approximately $ 4-billion in 2025. We consider relevant financial and policy incentives in funding the pipeline network construction and establish both privately-funded and publicly-funded scenarios. Under the privately-funded scenario, we find that a private consortium taking advantage of the federal CCUS Tax Credit can achieve a target internal rate of return of 8% by charging $ 7.90/tonne of CO_2 transported over a 50-year period, or by charging $ 8.13/tonne of CO_2 transported over a 20-year period. Furthermore, we identify the Net Zero Accelerator initiative as a potential funding source, and the federal carbon pricing mechanism and the sequestration credit as policies that can propel the establishment of the CCS hub. Our work provides a comprehensive framework upon which additional CCS projects can be evaluated. The use of this framework, which considers each of the many factors that can affect the viability of a CCS system, is necessary to ensure the long-term success of CCS as a climate change mitigation tool.

CRediT authorship contribution statement

Yu Hao Zhao: Formal analysis, Investigation, Visualization, Writing – original draft. **Nima Shakourifar:** Methodology, Software, Writing – original draft. **Negar Shahsavar:** Methodology. **Yaxuan Lei:** Methodology, Software. **Benzhong Zhao:** Funding acquisition, Methodology, Project administration, Software, Supervision, Writing – review & editing.

Declaration of competing interest

The authors declare that they have no known competing financial interests or personal relationships that could have appeared to influence the work reported in this paper.

Data availability

Data will be made available on request.

Acknowledgements

This research was supported by the Natural Sciences and Engineering Research Council of Canada (NSERC) Discovery Grants (Grant RGPIN-2019-07162).

Appendix A. Supplementary data

Supplementary material related to this article can be found online at https://doi.org/10.1016/j.ijggc.2024.104129.

References

AER, 1994. Directive 051: Injection and disposal wells.
Alberta Department of Energy, 2020. Quest Carbon Capture and Storage Project Annual Summary Report. Report, URL: https://open.alberta.ca/dataset/f74375f3-3c73-4b9c-af2b-ef44e59b7890/resource/ff260985-e616-4d2e-92e0-9b91f5590136/download/energy-quest-annual-summary-alberta-department-of-energy-2019.pdf.
Alberta Energy Regulator, 2023. CO_2 sequestration. URL: https://www.aer.ca/co2-sequestration.
Alberta Geological Survey, 1994a. Atlas of the Western Canada Sedimentary Basin: Chapter 12 - Devonian Woodbend-Winterburn Strata. Technical Report, Alberta Energy Regulator.
Alberta Geological Survey, 1994b. Atlas of the western Canada sedimentary basin: Chapter 13 - Devonian Wabamun group.
Alberta Geological Survey, Alberta Energy Regulator, 2021. Geological framework of alberta.
Alcalde, J., Heinemann, N., Mabon, L., Worden, R.H., de Coninck, H., Robertson, H., Maver, M., Ghanbari, S., Swennenhuis, F., Mann, I., Walker, T., Gomersal, S., Bond, C.E., Allen, M.J., Haszeldine, R.S., James, A., Mackay, E.J., Brownsort, P.A., Faulkner, D.R., Murphy, S., 2019. Acorn: Developing full-chain industrial carbon capture and storage in a resource- and infrastructure-rich hydrocarbon province. J. Clean. Prod. 233, 963–971. http://dx.doi.org/10.1016/j.jclepro.2019.06.087, URL: https://www.sciencedirect.com/science/article/pii/S0959652619320426.

Anderson, S., Newell, R., 2004. Prospects for carbon capture and storage technologies. Annu. Rev. Environ. Resour. 29 (1), 109–142. http://dx.doi.org/10.1146/annurev.energy.29.082703.145619.

Ashrafi, O., Zamor, O., Navarri, P., 2021. Impact of carbon capture technologies on GHG emissions from oil sands in-situ facilities: A system prospective. Appl. Therm. Eng. 188, 116603. http://dx.doi.org/10.1016/j.applthermaleng.2021.116603.

Bachu, S., 2007. Carbon dioxide storage capacity in uneconomic coal beds in alberta, Canada: Methodology, potential and site identification. Int. J. Greenh. Gas Control 1 (3), 374–385. http://dx.doi.org/10.1016/S1750-5836(07)00070-9, URL: https://www.sciencedirect.com/science/article/pii/S1750583607000709.

Bachu, S., 2015. Review of CO_2 storage efficiency in deep saline aquifers. Int. J. Greenh. Gas Control 40, 188–202. http://dx.doi.org/10.1016/j.ijggc.2015.01.007, URL: https://www.sciencedirect.com/science/article/pii/S1750583615000146.

Bachu, S., 2016. Identification of oil reservoirs suitable for CO2-EOR and CO2 storage (CCUS) using reserves databases, with application to Alberta, Canada. Int. J. Greenh. Gas Control 44, 152–165.

Bachu, S., Bistran, R., Jafari, A., 2014a. Identification of Options for CO_2 Storage in the Athabasca Area, Alberta. Alberta Innovates.

Bachu, S., Melnik, A., Bistran, R., 2014b. Approach to evaluating the CO_2 storage capacity in devonian deep saline aquifers for emissions from oil sands operations in the Athabasca area, Canada. Energy Procedia 63, 5093–5102. http://dx.doi.org/10.1016/j.egypro.2014.11.539.

Bäckstrand, K., Meadowcroft, J., Oppenheimer, M., 2011. The politics and policy of carbon capture and storage: Framing an emergent technology. Global Environ. Change 21 (2), 275–281. http://dx.doi.org/10.1016/j.gloenvcha.2011.03.008, URL: https://www.sciencedirect.com/science/article/pii/S0959378011000355.

Balaji, K., Rabiei, M., 2022. Carbon dioxide pipeline route optimization for carbon capture, utilization, and storage: A case study for north-central USA. Sustain. Energy Technol. Assess. 51, 101900. http://dx.doi.org/10.1016/J.SETA.2021.101900.

Bandilla, K.W., Guo, B., Celia, M.A., 2019. A guideline for appropriate application of vertcially-integrated modeling approaches for geologic carbon storage modeling. Int. J. Greenh. Gas Control 91, 102808.

Bank of Canada, 2016. Renewal of the inflation-control target. URL: https://www.bankofcanada.ca/wp-content/uploads/2016/10/background_nov11.pdf.

Bank of Canada, 2022. Annual exchange rates.

Bell, J., Bachu, S., 2003. In situ stress magnitude and orientation estimates for Cretaceous coal-bearing strata beneath the plains area of central and southern Alberta. Bull. Can. Pet. Geol. 51 (1), 1–28. http://dx.doi.org/10.2113/gscpgbull.51.1.1.

Bennion, D.B., Bachu, S., 2008. Drainage and imbibition relative permeability relationships for supercritical CO_2/brine and H_2S/brine systems in intergranular sandstone, carbonate, shale, and anhydrite rocks. SPE Reserv. Eval. Eng. 11 (03), 487–496.

Boot-Handford, M.E., Abanades, J.C., Anthony, E.J., Blunt, M.J., Brandani, S., Mac Dowell, N., Fernández, J.R., Ferrari, M.-C., Gross, R., Hallett, J.P., Haszeldine, R.S., Heptonstall, P., Lyngfelt, A., Makuch, Z., Mangano, E., Porter, R.T.J., Pourkashanian, M., Rochelle, G.T., Shah, N., Yao, J.G., Fennell, P.S., 2014. Carbon capture and storage update. Energy Environ. Sci. 7 (1), 130–189. http://dx.doi.org/10.1039/C3EE42350F.

Budinis, S., Krevor, S., Dowell, N.M., Brandon, N., Hawkes, A., 2018. An assessment of CCS costs, barriers and potential. Energy Strategy Rev. 22, 61–81. http://dx.doi.org/10.1016/j.esr.2018.08.003, URL: https://www.sciencedirect.com/science/article/pii/S2211467X18300634.

Bui, M., Adjiman, C.S., Bardow, A., Anthony, E.J., Boston, A., Brown, S., Fennell, P.S., Fuss, S., Galindo, A., Hackett, L.A., Hallett, J.P., Herzog, H.J., Jackson, G., Kemper, J., Krevor, S., Maitland, G.C., Matuszewski, M., Metcalfe, I.S., Petit, C., Puxty, G., Reimer, J., Reiner, D.M., Rubin, E.S., Scott, S.A., Shah, N., Smit, B., Trusler, J.P.M., Webley, P., Wilcox, J., Mac Dowell, N., 2018. Carbon capture and storage (CCS): the way forward. Energy Environ. Sci. 11 (5), 1062–1176. http://dx.doi.org/10.1039/C7EE02342A.

Bureau of Labor Statistics, 2022. CPI inflation calculator.

Burton, M., Kumar, N., Bryant, S.L., 2009. CO_2 injectivity into brine aquifers: Why relative permeability matters as much as absolute permeability. Energy Procedia 1 (1), 3091–3098. http://dx.doi.org/10.1016/j.egypro.2009.02.089.

CAPP, 2021. Oil sands production. URL: https://www.capp.ca/resources/statistics/.

Chao, C., Deng, Y., Dewil, R., Baeyens, J., Fan, X., 2021. Post-combustion carbon capture. Renew. Sustain. Energy Rev. 138, http://dx.doi.org/10.1016/j.rser.2020.110490, 110490–110490. URL: https://www.sciencedirect.com/science/article/pii/S1364032120307760.

Ciotta, M., Peyerl, D., Zacharias, L.G.L., Fontenelle, A.L., Tassinari, C., Moretto, E.M., 2021. CO_2 storage potential of offshore oil and gas fields in Brazil. Int. J. Greenh. Gas Control 112, http://dx.doi.org/10.1016/j.ijggc.2021.103492, 103492–103492. URL: https://www.sciencedirect.com/science/article/pii/S1750583621002449.

Clark, A.J., Lake, L.W., Patzek, T.W., 2011. Production forecasting with logistic growth models. Proc. - SPE Annu. Tech. Conf. Exhib. 1, 184–194. http://dx.doi.org/10.2118/144790-MS.

Cole, S., Itani, S., 2013. The alberta carbon trunk line and the benefits of CO_2. Energy Procedia 37, 6133–6139. http://dx.doi.org/10.1016/j.egypro.2013.06.542, URL: https://www.sciencedirect.com/science/article/pii/S1876610213007856.

Department of Finance Canada, 2022. Legislative proposals relating to income tax and other legislation.

Department of the Environment, 2020. Clean fuel regulations. URL: https://gazette.gc.ca/rp-pr/p1/2020/2020-12-19/html/reg2-eng.html.

Duong, C., Bower, C., Hume, K., Rock, L., Tessarolo, S., 2019. Quest carbon capture and storage offset project: Findings and learnings from 1st reporting period. Int. J. Greenh. Gas Control 89, 65–75. http://dx.doi.org/10.1016/j.ijggc.2019.06.001, URL: https://www.sciencedirect.com/science/article/pii/S1750583618307904.

Edwards, R.W.J., Celia, M.A., 2018. Infrastructure to enable deployment of carbon capture, utilization, and storage in the United States. Proc. Natl. Acad. Sci. 115 (38), E8815–E8824. http://dx.doi.org/10.1073/pnas.1806504115, URL: https://www.pnas.org/content/pnas/115/38/E8815.full.pdf.

Eisinger, C.L., Lavoie, R., Keith, D.W., 2011. The Wabamun Area sequestration project (WASP): A multidisciplinary study of gigaton scale CO_2 storage in a deep saline carbonate aquifer. Energy Procedia 4, 4793–4797. http://dx.doi.org/10.1016/j.egypro.2011.02.444, URL: https://www.sciencedirect.com/science/article/pii/S1876610211007235.

Environment and Climate Change Canada, 2020. A healthy environment and a healthy economy. URL: https://www.canada.ca/content/dam/eccc/documents/pdf/climate-change/climate-plan/healthy_environment_healthy_economy_plan.pdf.

Environment and Climate Change Canada, 2021a. Annex: Modelling and analysis of a healthy environment and a healthy economy. URL: https://www.canada.ca/en/services/environment/weather/climatechange/climate-plan/climate-plan-overview/healthy-environment-healthy-economy/annex-modelling-analysis.html.

Environment and Climate Change Canada, 2021b. Canada's climate actions for a healthy environment and a healthy economy. URL: https://www.canada.ca/en/services/environment/weather/climatechange/climate-plan/climate-plan-overview/actions-healthy-environment-economy.html.

Environment and Climate Change Canada, 2021c. Greenhouse gas sources and sinks: Executive summary 2021. URL: https://www.canada.ca/en/environment-climate-change/services/climate-change/greenhouse-gas-emissions/sources-sinks-executive-summary-2021.html#toc2.

Environment and Climate Change Canada, 2021d. Progress towards Canada's greenhouse gas emissions reduction target. URL: https://www.canada.ca/en/environment-climate-change/services/environmental-indicators/progress-towards-canada-greenhouse-gas-emissions-reduction-target.html.

Environment and Climate Change Canada, 2022. 2030 Emissions reduction plan.

Falkowski, P., Scholes, R.J., Boyle, E., Canadell, J., Canfield, D., Elser, J., Gruber, N., Hibbard, K., Högberg, P., Linder, S., Mackenzie, F.T., Moore, B.I.I.I., Pedersen, T., Rosenthal, Y., Seitzinger, S., Smetacek, V., Steffen, W., 2000. The global carbon cycle: A test of our knowledge of earth as a system. Science 290 (5490), 291–296. http://dx.doi.org/10.1126/science.290.5490.291.

Ghaderi, S., Leonenko, Y., 2015. Reservoir modeling for wabamun lake sequestration project. Energy Sci. Eng..

Goodarzi, S., Settari, A., Keith, D., 2012. Geomechanical modeling for CO_2 storage in nisku aquifer in Wabamun Lake area in Canada. Int. J. Greenh. Gas Control 10, 113–122.

Goodman, A., Hakala, A., Bromhal, G., Deel, D., Rodosta, T., Frailey, S., Small, M., Allen, D., Romanov, V., Fazio, J., Huerta, N., McIntyre, D., Kutchko, B., Guthrie, G., 2011. U.S. DOE methodology for the development of geologic storage potential for carbon dioxide at the national and regional scale. Int. J. Greenh. Gas Control 5 (4), 952–965. http://dx.doi.org/10.1016/j.ijggc.2011.03.010, URL: https://www.sciencedirect.com/science/article/pii/S1750583611000405.

Government of Alberta, 2011. Carbon sequestration tenure regulation.

Government of Alberta, 2020. Technology innovation and emissions reduction regulation. URL: https://www.qp.alberta.ca/1266.cfm?page=2019_133.cfm&leg_type=Regs&isbncln=9780779818501.

Government of Alberta, 2021. Request for full project proposals for carbon sequestration hubs. URL: https://www.alberta.ca/assets/documents/energy-request-for-full-project-proposals-rfpp-guidelines.pdf.

Government of Canada, 2021a. Budget 2021. URL: https://www.budget.gc.ca/2021/home-accueil-en.html.

Government of Canada, 2021b. Greenhouse gas reporting program (GHGRP) - facility greenhouse gas (GHG) data. URL: https://open.canada.ca/data/en/dataset/a8ba14b7-7f23-462a-bdbb-83b0ef629823.

Government of Canada, 2021c. Net zero accelerator initiative - strategic innovation fund. URL: https://www.ic.gc.ca/eic/site/125.nsf/eng/00039.html.

Government of Canada, 2021d. Net-zero emissions by 2050. URL: https://www.canada.ca/en/services/environment/weather/climatechange/climate-plan/net-zero-emissions-2050.html.

Government of Canada, 2022. What is the clean fuel standard? URL: https://www.canada.ca/en/environment-climate-change/services/managing-pollution/energy-production/fuel-regulations/clean-fuel-standard/about.html#toc0.

Hansen, J., Sato, M., 2004. Greenhouse gas growth rates. Proc. Natl. Acad. Sci. USA 101 (46), 16109–16114. http://dx.doi.org/10.1073/pnas.0406982101, URL: https://www.pnas.org/content/pnas/101/46/16109.full.pdf.

Hasan, M.M.F., First, E.L., Boukouvala, F., Floudas, C.A., 2015. A multi-scale framework for CO_2 capture, utilization, and sequestration: CCUS and CCU. Comput. Chem. Eng. 81, 2–21. http://dx.doi.org/10.1016/j.compchemeng.2015.04.034, URL: https://www.sciencedirect.com/science/article/pii/S0098135415001350.

Haszeldine, R.S., 2009. Carbon capture and storage: How green can black be? Science 325 (5948), 1647–1652. http://dx.doi.org/10.1126/science.1172246, URL: https://www.science.org/doi/abs/10.1126/science.1172246.

Heddle, G., Herzog, H., Klett, M., 2003. The Economics of CO_2 Storage. Report, URL: http://lfee.mit.edu/publications/.

Heidaryan, E., Hatami, T., Rahimi, M., Moghadasi, J., 2011. Viscosity of pure carbon dioxide at supercritical region: Measurement and correlation approach. J. Supercrit. Fluids 56, 144–151. http://dx.doi.org/10.1016/J.SUPFLU.2010.12.006.

Hesse, M.A., Orr, Jr., F.M., Tchelepi, H.A., 2008. Gravity currents with residual trapping. 611, 35–60.

Hidalgo, J.J., MacMinn, C.W., Juanes, R., 2013. Dynamics of convective dissolution from a migrating current of carbon dioxide. Adv. Water Resour. 62, 511–519.

Hubbert, M.K., 1956. Nuclear Energy and the Fossil Fuels. Report, URL: http://www.energycrisis.com/Hubbert/1956/1956.pdf.

Infrastructure Canada, 2016. Infrastructure Canada projects since 2002 - national.

Infrastructure Canada, 2022. Investing in Canada plan – building a better Canada. URL: https://www.infrastructure.gc.ca/plan/about-invest-apropos-eng.html.

International Energy Agency, 2020. CCUS in Clean Energy Transitions. Report, URL: https://www.iea.org/reports/ccus-in-clean-energy-transitions.

Jensen, M.D., Pei, P., Snyder, A.C., Heebink, L.V., Gorecki, C.D., Steadman, E.N., Harju, J.A., 2013. A phased approach to building a hypothetical pipeline network for CO_2 transport during CCUS. Energy Procedia 37, 3097–3104. http://dx.doi.org/10.1016/j.egypro.2013.06.195, URL: https://www.sciencedirect.com/science/article/pii/S1876610213004384.

Juanes, R., MacMinn, C.W., Szulczewski, M.L., 2010. The footprint of the CO_2 plume during carbon dioxide storage in saline aquifers: storage efficiency for capillary trapping at the basin scale. Transp. Porous Media 82 (1), 19–30.

Kazemifar, F., 2021. A review of technologies for carbon capture, sequestration, and utilization: Cost, capacity, and technology readiness. Greenh. Gas.: Sci. Technol. http://dx.doi.org/10.1002/GHG.2131, URL: https://onlinelibrary.wiley.com/doi/full/10.1002/ghg.2131https://onlinelibrary.wiley.com/doi/abs/10.1002/ghg.2131https://onlinelibrary.wiley.com/doi/10.1002/ghg.2131.

Kennedy, C., Steinberger, J., Gasson, B., Hansen, Y., Hillman, T., Havránek, M., Pataki, D., Phdungsilp, A., Ramaswami, A., Mendez, G.V., 2009. Greenhouse gas emissions from global cities. Environ. Sci. Technol. 43 (19), 7297–7302. http://dx.doi.org/10.1021/es900213p.

Klyukin, Y.I., Lowell, R.P., Bodnar, R.J., 2017. A revised empirical model to calculate the dynamic viscosity of H_2O NaCl fluids at elevated temperatures and pressures (≤1000 °C, ≤500 MPa, 0–100 wt % NaCl). Fluid Phase Equilib. 433, 193–205. http://dx.doi.org/10.1016/j.fluid.2016.11.002.

Kuby, M.J., Middleton, R.S., Bielicki, J.M., 2011. Analysis of cost savings from networking pipelines in CCS infrastructure systems. Energy Procedia 4, 2808–2815. http://dx.doi.org/10.1016/J.EGYPRO.2011.02.185.

Lackner, K.S., 2003. A guide to CO_2 sequestration. Science 300 (5626), 1677–1678. http://dx.doi.org/10.1126/science.1079033, URL: https://www.science.org/doi/abs/10.1126/science.1079033.

Leonzio, G., Foscolo, P.U., Zondervan, E., 2019. An outlook towards 2030: Optimization and design of a CCUS supply chain in Germany. Comput. Chem. Eng. 125, 499–513. http://dx.doi.org/10.1016/j.compchemeng.2019.04.001, URL: https://www.sciencedirect.com/science/article/pii/S0098135418310883.

Leung, D.Y.C., Caramanna, G., Maroto-Valer, M.M., 2014. An overview of current status of carbon dioxide capture and storage technologies. Renew. Sustain. Energy Rev. 39, 426–443. http://dx.doi.org/10.1016/j.rser.2014.07.093, URL: https://www.sciencedirect.com/science/article/pii/S1364032114005450.

Liang, Z., Rongwong, W., Liu, H., Fu, K., Gao, H., Cao, F., Zhang, R., Sema, T., Henni, A., Sumon, K., Nath, D., Gelowitz, D., Srisang, W., Saiwan, C., Benamor, A., Al-Marri, M., Shi, H., Supap, T., Chan, C., Zhou, Q., Abu-Zahra, M., Wilson, M., Olson, W., Idem, R., Tontiwachwuthikul, P., 2015. Recent progress and new developments in post-combustion carbon-capture technology with amine based solvents. Int. J. Greenh. Gas Control 40, 26–54. http://dx.doi.org/10.1016/J.IJGGC.2015.06.017, (Henry) (PT).

MacDowell, N., Florin, N., Buchard, A., Hallett, J., Galindo, A., Jackson, G., Adjiman, C.S., Williams, C.K., Shah, N., Fennell, P., 2010. An overview of CO_2 capture technologies. Energy Environ. Sci. 3 (11), 1645–1669. http://dx.doi.org/10.1039/C004106H, URL: https://pubs.rsc.org/en/content/articlehtml/2010/ee/c004106h.

MacMinn, C.W., Szulczewski, M.L., Juanes, R., 2011. CO_2 migration in saline aquifers. Part 2: Capillary and solubility trapping. J. Fluid Mech. 688 (321–351).

McCollum, D., Ogden, J., 2006. Techno-Economic Models for Carbon Dioxide Compression, Transport, and Storage and Correlations for Estimating Carbon Dioxide Density and Viscosity. Report, URL: https://itspubs.ucdavis.edu/publication_detail.php?id=1047.

McCoy, S.T., Rubin, E.S., 2008. An engineering-economic model of pipeline transport of CO_2 with application to carbon capture and storage. Int. J. Greenh. Gas Control 2 (2), 219–229. http://dx.doi.org/10.1016/S1750-5836(07)00119-3, URL: https://www.sciencedirect.com/science/article/pii/S1750583607001193.

Metz, B., Davidson, O., De Coninck, H., Loos, M., Meyer, L., 2005. IPCC Special Report on Carbon Dioxide Capture and Storage. Cambridge University Press, Cambridge.

Mokhtar, M., Ali, M.T., Khalilpour, R., Abbas, A., Shah, N., Hajaj, A.A., Armstrong, P., Chiesa, M., Sgouridis, S., 2012. Solar-assisted post-combustion carbon capture feasibility study. Appl. Energy 92, 668–676. http://dx.doi.org/10.1016/J.APENERGY.2011.07.032.

National Energy Technology Laboratory, 2018. FE/NETL CO_2 Transport Cost Model. Technical Report, US Department of Energy National Energy Technology Laboratory, Pittsburgh.

Nicot, J.-P., 2008. Evaluation of large-scale CO_2 storage on fresh-water sections of aquifers: An example from the Texas Gulf Coast basin. Int. J. Greenh. Gas Control 2 (4), 582–593.

Nordbotten, J.M., Celia, M.A., Bachu, S., 2005. Injection and storage of CO_2 in deep saline aquifers: Analytical solution for CO_2 plume evolution during injection. Transp. Porous Media 58 (3), 339–360.

NPC, 2019. Meeting the dual challenge: A roadmap to at-scale deployment of carbon capture, use, and storage. URL: https://dualchallenge.npc.org.

Nygaard, R., Lavoie, R., 2009. Wabamun Area CO_2 Sequestration Project ($WASP$). Technical Report, University of Calgary.

Ordorica-Garcia, G., Wong, S., Faltinson, J., 2011. Characterisation of CO_2 emissions in Canada's oil sands industry: Estimating the future CO_2 supply and capture cost curves. Energy Procedia 4, 2637–2644. http://dx.doi.org/10.1016/j.egypro.2011.02.163.

Orr, F.M., 2009. Onshore geologic storage of CO_2. Science 325, 1656–1658. http://dx.doi.org/10.1126/SCIENCE.1175677, URL: https://www.science.org/doi/abs/10.1126/science.1175677.

Osman, A.I., Hefny, M., Abdel Maksoud, M.I.A., Elgarahy, A.M., Rooney, D.W., 2021. Recent advances in carbon capture storage and utilisation technologies: a review. Environ. Chem. Lett. 19 (2), 797–849. http://dx.doi.org/10.1007/s10311-020-01133-3.

Ouyang, L.-B., 2011. New correlations for predicting the density and viscosity of supercritical carbon dioxide under conditions expected in carbon capture and sequestration operations. Open Pet. Eng. J. 4, 13–21.

Pacala, S., Socolow, R., 2004. Stabilization wedges: Solving the climate problem for the next 50 years with current technologies. Science 305 (5686), 968–972. http://dx.doi.org/10.1126/science.1100103, URL: https://www.science.org/doi/abs/10.1126/science.1100103.

Parker, N., 2004. Using Natural Gas Transmission Pipeline Costs to Estimate Hydrogen Pipeline Costs. Report, URL: https://itspubs.ucdavis.edu/publication_detail.php?id=197.

Parliamentary Budget Officer, 2022. Federal infrastructure spending, 2016-17 to 2026-27.

Pau, G.S., Bell, J.B., Pruess, K., Almgren, A.S., Lijewski, M.J., Zhang, K., 2010. High-resolution simulation and characterization of density-driven flow in CO_2 storage in saline aquifers. Adv. Water Resour. 33 (4), 443–455.

Peletiri, S.P., Rahmanian, N., Mujtaba, I.M., 2018. CO_2 pipeline design: A review. Energies 11 (9), http://dx.doi.org/10.3390/EN11092184, 2184–2184. 2018, Vol. 11, Page 2184. URL: https://www.mdpi.com/1996-1073/11/9/2184/htmhttps://www.mdpi.com/1996-1073/11/9/2184.

Pilorgé, H., McQueen, N., Maynard, D., Psarras, P., He, J., Rufael, T., Wilcox, J., 2020. Cost analysis of carbon capture and sequestration of process emissions from the U.S. industrial sector. Environ. Sci. Technol. 54 (12), 7524–7532. http://dx.doi.org/10.1021/acs.est.9b07930.

Pinder, G.F., Gray, W.G., 2008. Essentials of Multiphase Flow and Transport in Porous Media.

Porter, R.T.J., Fairweather, M., Kolster, C., Mac Dowell, N., Shah, N., Woolley, R.M., 2017. Cost and performance of some carbon capture technology options for producing different quality CO_2 product streams. Int. J. Greenh. Gas Control 57, 185–195. http://dx.doi.org/10.1016/j.ijggc.2016.11.020.

Potkins, M., 2022. Alberta's industrial carbon tax to triple by 2030 to match Ottawa's minimum standards. URL: https://financialpost.com/commodities/energy/alberta-carbon-tax-triple-federal-emissions-pricing-schedule.

Ranaee, E., Khattar, R., Inzoli, F., Blunt, M.J., Guadagnini, A., 2022. Assessment and uncertainty quantification of onshore geological CO_2 storage capacity in China. Int. J. Greenh. Gas Control 121, 103804.

Raza, A., Gholami, R., Rezaee, R., Rasouli, V., Rabiei, M., 2019. Significant aspects of carbon capture and storage – A review. Petroleum 5 (4), 335–340. http://dx.doi.org/10.1016/j.petlm.2018.12.007.

Ringrose, P.S., Furre, A.-K., Gilfillan, S.M., Krevor, S., Landrø, M., Leslie, R., Meckel, T., Nazarian, B., Zahid, A., 2021. Storage of carbon dioxide in saline aquifers: Physicochemical processes, key constraints, and scale-up potential. Annu. Rev. Chem. Biomol. Eng. 12 (1), 471–494. http://dx.doi.org/10.1146/annurev-chembioeng-093020-091447.

Rockström, J., Steffen, W., Noone, K., Persson, Å., Chapin, F.S., Lambin, E.F., Lenton, T.M., Scheffer, M., Folke, C., Schellnhuber, H.J., Nykvist, B., de Wit, C.A., Hughes, T., van der Leeuw, S., Rodhe, H., Sörlin, S., Snyder, P.K., Costanza, R., Svedin, U., Falkenmark, M., Karlberg, L., Corell, R.W., Fabry, V.J., Hansen, J., Walker, B., Liverman, D., Richardson, K., Crutzen, P., Foley, J.A., 2009. A safe operating space for humanity. Nature 461 (7263), 472–475. http://dx.doi.org/10.1038/461472a.

Romasheva, N., Ilinova, A., 2019. CCS projects: How regulatory framework influences their deployment. Resources 8 (4), http://dx.doi.org/10.3390/resources8040181, 181–181. URL: https://www.mdpi.com/2079-9276/8/4/181.

Skagestad, R., Lach, A., kke, N.R., Eldrup, N.H., 2014. Critical factors influencing CO_2 capture cost, a case study. Energy Procedia 63, 7298–7306. http://dx.doi.org/10.1016/j.egypro.2014.11.766.

Smith, E., Morris, J., Kheshgi, H., Teletzke, G., Herzog, H., Paltsev, S., 2021. The cost of CO_2 transport and storage in global integrated assessment modeling. Int. J. Greenh. Gas Control 109, 103367. http://dx.doi.org/10.1016/J.IJGGC.2021.103367.

Sorrell, S., Speirs, J., 2019. UKERC Review of Evidence for Global Oil Depletion. Technical Report 5: Methods of Estimating Ultimately Recoverable Resources. Report, URL: https://ukerc8.dl.ac.uk/UCAT/PUBLICATIONS/UKERC_Review_of_Evidence_on_Global_Oil_Depletion-Technical_Report_5-Methods_of_estimating_ultimately_recoverable_resources.pdf.

Szulczewski, M.L., Macminn, C.W., Herzog, H.J., Juanes, R., 2012. Lifetime of carbon capture and storage as a climate-change mitigation technology. Proc. Natl. Acad. Sci. 109 (14), 5185–5189. http://dx.doi.org/10.1073/pnas.1115347109.

Szulczewski, M.L., MacMinn, C.W., Juanes, R., 2014. Theoretical analysis of how pressure buildup and CO_2 migration can both constrain storage capacity in deep saline aquifers. Int. J. Greenh. Gas Control 23, 113–118.

Tapia, J.F.D., Lee, J.-Y., Ooi, R.E.H., Foo, D.C.Y., Tan, R.R., 2018. A review of optimization and decision-making models for the planning of CO_2 capture, utilization and storage (CCUS) systems. Sustain. Prod. Consump. 13, 1–15. http://dx.doi.org/10.1016/j.spc.2017.10.001.

United Nations, 2015. Paris agreement. URL: https://unfccc.int/sites/default/files/english_paris_agreement.pdf.

Weihs, G.A.F., Wiley, D.E., 2012. Steady-state design of CO_2 pipeline networks for minimal cost per tonne of CO_2 avoided. Int. J. Greenh. Gas Control 8, 150–168. http://dx.doi.org/10.1016/j.ijggc.2012.02.008.

WorleyParsons, 2003. Baseline Hydrogeology Assessment. Report, URL: https://open.alberta.ca/dataset/9625726c-66b5-4673-954a-8e96b67b6637/resource/f05520e4-01f6-43be-8708-7ddb3f03a395/download/BASELINE-HYDROGEOLOGY-ASSESSMENT.pdf.

Yao, X., Zhong, P., Zhang, X., Zhu, L., 2018. Business model design for the carbon capture utilization and storage (CCUS) project in China. Energy Policy 121, 519–533. http://dx.doi.org/10.1016/j.enpol.2018.06.019.

Yu, S., Horing, J., Liu, Q., Dahowski, R., Davidson, C., Edmonds, J., Liu, B., Mcjeon, H., McLeod, J., Patel, P., Clarke, L., 2019. CCUS in China's mitigation strategy: Insights from integrated assessment modeling. Int. J. Greenh. Gas Control 84, 204–218. http://dx.doi.org/10.1016/J.IJGGC.2019.03.004.

Zanco, S.E., Pérez-Calvo, J.-F., Gasós, A., Cordiano, B., Becattini, V., Mazzotti, M., 2021. Postcombustion CO_2 capture: A comparative techno-economic assessment of three technologies using a solvent, an adsorbent, and a membrane. ACS Eng. Au 1 (1), 50–72. http://dx.doi.org/10.1021/acsengineeringau.1c00002.